BIOCHEMISTRY
including biophysical chemistry & molecular biology

Article

pubs.acs.org/biochemistry

Determination of the Miss Probabilities of Individual S-State Transitions during Photosynthetic Water Oxidation by Monitoring Electron Flow in Photosystem II Using FTIR Spectroscopy

Hiroyuki Suzuki,[†] Miwa Sugiura,[‡,§] and Takumi Noguchi*[,†]

[†]Division of Material Science, Graduate School of Science, Nagoya University, Furo-cho, Chikusa-ku, Nagoya 464-8602, Japan
[‡]Cell-Free Science and Technology Research Center, Ehime University, Matsuyama, Ehime 790-8577, Japan
[§]PRESTO, Japan Science and Technology Agency (JST), 4-1-8, Honcho, Kawagchi, Saitama 332-0012, Japan

ABSTRACT: Water oxidation by plants and cyanobacteria is performed via a light-driven cycle of five intermediates called S states (S_0–S_4) at the water oxidizing center (WOC) in photosystem II (PSII). The information about misses, i.e., the probabilities that the S-state transitions failed to advance, is crucial for detailed analysis of various spectroscopic data in investigations of the water oxidation mechanism. In this study, we have determined the miss probabilities of the individual S-state transitions using light-induced Fourier transform infrared (FTIR) difference spectroscopy. The extent of S-state transitions in the WOC upon each saturating flash was monitored by detecting the flow of electrons from the WOC to ferricyanide, an exogenous electron acceptor, using the CN stretching bands of ferricyanide and ferrocyanide. Simulation of the oscillation pattern of the flash-number dependence of the signal amplitude provided the miss probabilities for the $S_0 \rightarrow S_1$, $S_1 \rightarrow S_2$, $S_2 \rightarrow S_3$, and $S_3 \rightarrow S_0$ transitions (α_0–α_3, respectively) without any assumption about fitting parameters. The results for PSII preparations from *Thermosynechococcus elongatus* and spinach showed a general tendency of misses in the order, $\alpha_0 \leq \alpha_1 < \alpha_2 < \alpha_3$, indicating that a more oxidized WOC has a higher miss probability. A very similar result observed for the Y_D-less mutant (D2-Y160F) of *T. elongatus* confirmed that Y_D does not affect the estimated misses. It was further shown that NO_3^- treatment specifically increased α_3, consistent with inactivation of the S_3 state reported previously. These results demonstrate the usefulness of this FTIR method for estimating individual miss probabilities in the S-state cycle in elucidation of the molecular mechanism of photosynthetic water oxidation.

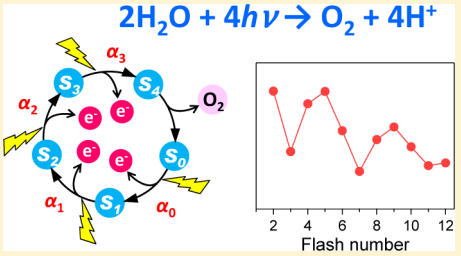

In oxygenic photosynthesis performed by plants and cyanobacteria, solar energy is converted to chemical energy by utilizing water as an ultimate electron donor to reduce CO_2. As a result of water oxidation, molecular oxygen is released to the atmosphere, which makes aerobic life on earth possible. The water oxidation takes place in photosystem II (PSII) protein complexes embedded in thylakoid membranes.[1−6] Upon illumination, charge separation takes place from the excited singlet state of chlorophyll, delocalized over the monomeric chlorophyll Chl_{D1} and the dimeric chlorophyll P680,[7] to produce a $P680^+Pheo^-$ charged pair.[8] On the electron acceptor side, the electron is transferred from $Pheo^-$ to the primary quinone electron acceptor Q_A and then to the secondary quinone Q_B.[9] On the donor side, $P680^+$ oxidizes Y_Z (D1-Tyr161) and then the water oxidizing center (WOC), which is the catalytic site of water oxidation.[1−6] The WOC consists of a Mn_4CaO_5 cluster and surrounding amino acid ligands to the Mn and Ca ions (six carboxylate groups and one imidazole group from the D1 and CP43 subunits).[10−13] The recent X-ray crystallographic structure at 1.9 Å resolution[12] also resolved four water oxygens ligated to the Mn cluster, which are candidates of substrates.

Water oxidation in the WOC requires abstraction of four electrons from two water molecules, i.e., four turnovers of electron transfer in PSII. Such four-electron reactions proceed through a cycle of five intermediates designated as S_i states (i = 0–4) (Figure 1).[14−16] When PSII is illuminated by a series of single-turnover flashes (strong enough to saturate PSII and short enough to allow only one charge separation), O_2 is released mainly on the 3rd flash and then every four flashes. This reflects the four-step oxidation of the WOC from the S_0

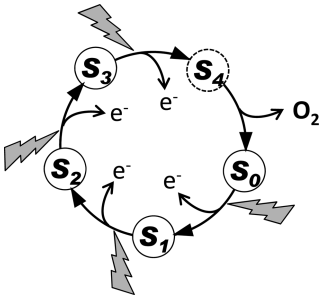

Figure 1. S-State cycle of photosynthetic water oxidation. Flash illumination advances the S_i state to the S_{i+1} state (i = 0–3), while the transient S_4 state relaxes to the S_0 state releasing molecular oxygen.

Received: May 30, 2012
Revised: August 9, 2012
Published: August 10, 2012

state to the S_4 state, which is reduced back to S_0 releasing O_2 (Figure 1). The maximal O_2 release at the 3rd flash indicates that the S_1 state, which is one-electron oxidized from the S_0 state, is the most stable in the dark.[16]

The period-four oscillation of O_2 evolution is damped as the flash number increases.[14−16] This is ascribed to the failures of S-state transitions, so-called misses, which are caused mainly by charge recombination between $P680^+$ and Q_A^- during the electron transfer process.[16−20] Double hits, which take place when microsecond flashes are used for excitation, also contribute to the damping,[15−20] although they can be eliminated by using short flashes such as nanosecond laser pulses.[21] It has been suggested that miss probabilities are different depending on the S-state transitions[18,19,22−25] because of the differences in the kinetics and equilibria in the components on the electron donor side.[24,26,27] Even the redox state of Q_B (Q_B or Q_B^-) affects the misses because of the change in the redox equilibrium between Q_A and Q_B.[23]

To elucidate the reaction mechanism of water oxidation, spectroscopic analyses of the structural changes in the WOC and the reactions of substrate water during the S-state cycle are essential. So far, various spectroscopic methods have been applied to the investigations of the S-state cycle, e.g., UV absorption,[28−30] X-ray absorption,[13,31,32] electron paramagnetic resonance,[25,33,34] mass spectrometry,[35] and infrared spectroscopy.[36−40] Starting from the S_1 state, the reaction cycle was stimulated by a train of flashes monitoring the spectroscopic signals. Because of the misses, however, the reactions after the 2nd flash always consist of the mixture of different S-state transitions. Thus, it is crucial to know the exact values of miss probabilities during the cycle to extract the contributions of pure S-state transitions from raw spectroscopic data for detailed and accurate analysis.

An average miss of the S-state transitions can be estimated from simulation of the oscillation pattern of the flash-number dependence of O_2 evolution[17,19,20] and that of other spectroscopic signals.[18,32,36,37,41] However, it has been difficult to estimate the probabilities of individual S-state transitions. Analysis of the O_2 pattern could only suggest the higher misses in the $S_2 \rightarrow S_3$ or $S_3 \rightarrow S_0$ transition.[18,19,22] De Wijn and van Gorkom[24] estimated individual miss probabilities by detecting fluorescence yield transitions. In simulations, however, some assumptions were necessary for parameters of fluorescence and an acceptor side status, and hence, a unique solution of misses was not obtained. Nevertheless, they evaluated the relative amplitudes of misses, in which the $S_3 \rightarrow S_0$ transition has the highest value and the $S_0 \rightarrow S_1$ transition has no miss probability. On the other hand, Han et al.[25] quantified the populations of the S_0−S_3 states after illumination with zero to six flashes on PSII membranes using the EPR signal specific to each state and estimated the miss probabilities of individual S-state transitions. The highest miss probability was found in the $S_2 \rightarrow S_3$ transition, whereas the $S_3 \rightarrow S_0$ transition showed a relatively low miss probability. This result was significantly different from that of the fluorescence study. Thus, a definitive conclusion about the relationship of the amplitudes of miss probabilities has not yet been reached, and hence, the development of another method for estimation of individual misses is urgent.

In this study, we have determined the probabilities of all four flash-induced S-state transitions using FTIR difference spectroscopy. Previous FTIR studies were able to provide only an average miss probability using protein bands, because of the unknown signal intensities of individual S-state transitions.[36,37,42] Here, we monitored an electron flow in PSII by detecting the reaction of ferricyanide, an exogenous electron acceptor contained in samples, using the CN stretching bands of ferricyanide and ferrocyanide. Because the amplitude of the ferricyanide/ferrocyanide signal directly reflects the extent of electron flow from the WOC to ferricyanide irrespective of the S states in WOC, its flash-number dependence was simulated to provide the miss probabilities of individual transitions. We have applied this method to determine the miss probabilities in the core complexes of *Thermosynechococcus elongatus* (wild type and Y_D-less mutant) and PSII membranes of spinach. The PSII sample treated with NO_3^-, which is known to inactivate the S_3 state and retard the $S_3 \rightarrow S_0$ transition,[43,44] was also subjected to the analysis. The results well demonstrated that this method is effective for detailed analysis of the S-state cycle and hence quite useful in the investigation of the reaction mechanism of photosynthetic water oxidation.

MATERIALS AND METHODS

Samples. The PSII core complexes from the *T. elongatus* 43-H strain (designated as WT′ hereafter), in which the carboxyl terminus of the CP43 subunit was genetically histidine-tagged,[45] and its Y_D-less mutant (D2-Y160F)[46] were purified using Ni^{2+}-affinity column chromatography as described previously.[45,46] Oxygen-evolving PSII membranes from spinach[47] were prepared as reported previously.[48]

For FTIR measurements, PSII core complexes from *T. elongatus* (∼10 mg of Chl/mL) were suspended in 200 mM Mes-NaOH buffer (pH 6.0) containing 5 mM NaCl, 5 mM $CaCl_2$, and 0.06% *n*-dodecyl *β*-D-maltoside in the presence of 100 mM potassium ferricyanide and sandwiched with a pair of CaF_2 plates (25 mm in diameter) as described previously.[42] This high concentration of buffer was used to prevent a decrease in pH by protons released from the WOC, and it has been demonstrated that this concentration does not affect the S-state cycling.[42] To investigate the effect of NO_3^- treatment, the core complexes from *T. elongatus* WT′ were suspended in 200 mM Mes-NaOH buffer (pH 6.0) containing 20 mM $NaNO_3$, 10 mM $Ca(NO_3)_2$, and 0.06% *n*-dodecyl *β*-D-maltoside in the presence of 100 mM potassium ferricyanide (final concentration of NO_3^- of 40 mM).

PSII membranes of spinach (0.5 mg of Chl/mL) were suspended in a Mes buffer at pH 6.0 (40 mM Mes-NaOH, 400 mM sucrose, 5 mM NaCl, and 5 mM $CaCl_2$) in the presence of 20 mM potassium ferricyanide and centrifuged at 170000*g* for 40 min. In this case, a high concentration of buffer was avoided to prevent the release of the PsbP and PsbQ extrinsic proteins, which are necessary to achieve a high O_2 evolution activity, because of the high salt concentration. The resulting pellet was sandwiched between two CaF_2 plates. These sample cells were sealed with silicone grease.[37] The sample temperature was maintained at 10 °C by circulating cold water in a copper holder.

FTIR Measurements. Flash-induced FTIR difference spectra were measured on a Bruker IFS-66/S spectrophotometer equipped with an MCT detector (InfraRed D316/8) at 4 cm^{-1} resolution.[49] Flash illumination was performed by a Q-switched Nd:YAG laser (Quanta-Ray GCR-130, 532 nm, ∼7 ns full width at half-maximum) with a power of ∼7 mJ cm^{-1} $pulse^{-1}$ at the sample point, which was strong enough to saturate the electron transfer reaction. The PSII core sample of *T. elongatus* was illuminated by two preflashes (1 s interval) and

dx.doi.org/10.1021/bi300708a | *Biochemistry* 2012, 51, 6776−6785

then dark adapted for 30 min. This procedure synchronizes the S states of all centers to the S_1 state. Twelve flashes were then applied to the sample at intervals of 20 s, and single-beam spectra (40 scans, 20 s scan) were measured before the 1st flash, between the flashes, and after the 12th flash. The sample was then dark adapted for 30 min again. This entire process was repeated six times, and the spectra were averaged to calculate flash-induced difference spectra. Spectra were measured using two different samples to obtain final average data. The similar measurement scheme was used for the PSII membranes of spinach. In this case, however, dark incubation was performed for 20 min and the interval of flashes and hence the measurement duration was 10 s. The cycle was repeated three times, and the data were averaged.

Data Analysis. The amplitude of the CN stretching bands of ferricyanide and ferrocyanide at 2116 and 2038 cm^{-1}, respectively, was estimated by fitting of the spectrum between 2160 and 1970 cm^{-1} using an average spectrum of the 1st to 12th flash spectra. The amplitude of protein bands was estimated as the ΔA at 1400 cm^{-1} relative to that at 1438 cm^{-1} in the carboxylate stretching region. Spectral fitting and simulation of the oscillation pattern were performed using Igor Pro (WaveMetrics Inc.).

RESULTS

Flash-induced FTIR difference spectra of the S-state cycle were measured by applying 12 successive flashes on the PSII core complexes of *T. elongatus* WT′ in the presence of ferricyanide as an exogenous electron acceptor. Figure 2 presents the spectra at the 1st (a), 2nd (b), 3rd (c), and 4th (d) flashes, of the 12 obtained spectra, with major contributions from the $S_1 \rightarrow S_2$, $S_2 \rightarrow S_3$, $S_3 \rightarrow S_0$, and $S_0 \rightarrow S_1$ transitions, respectively.[36,37] In these spectra, sharp prominent peaks appeared at 2116 and 2038 cm^{-1} that are attributed to the CN stretching vibrations of ferricyanide and ferrocyanide, respectively, indicative of electron abstraction by ferricyanide on the electron acceptor side. The much stronger intensity of ferrocyanide at 2038 cm^{-1} versus that of ferricyanide at 2116 cm^{-1} is attributed to the extinction coefficient that is originally larger in the former absorption.[50] Numerous protein bands are observed below 1750 cm^{-1}. Bands in the 1600−1450 and 1450−1300 cm^{-1} regions are typical of asymmetric and symmetric stretching vibrations, respectively, of carboxylate groups from Asp, Glu, and the C-terminus.[51−56] Bands in the 1700−1600 cm^{-1} region are mostly attributed to the amide I vibrations of polypeptide chains (CO stretches of backbone amides), while the amide II vibrations (NH bend + CN stretch of backbone amides) also contribute to the bands around 1550 cm^{-1}.[52,53] Signals of other amino acid side chains such as His (1120−1110 cm^{-1})[39,57] and Arg (1700−1550 cm^{-1})[58] have also been identified. The spectral features in the protein region (<1750 cm^{-1}) are significantly different among the four spectra, confirming the detection of four different S-state transitions.[36,37] In addition, reactions of water molecules have been detected in the OH stretching region (>3000 cm^{-1}),[59] while the structural changes of the Mn_4CaO_5 core have been observed as the Mn−O−Mn vibrations in a low-frequency region (650−600 cm^{-1}).[60,61] It is of particular importance that any vibrations from proteins, water, and the Mn_4CaO_5 core do not superimpose with the region of the ferricyanide and ferrocyanide CN vibrations at 2116 and 2038 cm^{-1}, respectively, and hence, the amplitudes of ferricyanide and ferrocyanide signals can be accurately estimated from the spectra.[a]

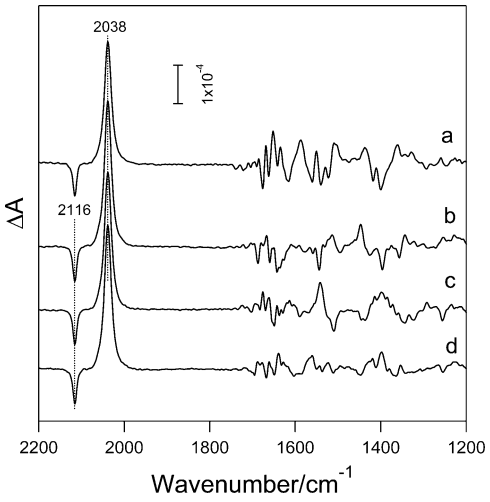

Figure 2. Flash-induced FTIR difference spectra of the S-state cycle in the core complexes of *T. elongatus* WT′: (a) 1st flash, (b) 2nd flash, (c) 3rd flash, and (d) 4th flash. The sample temperature was 10 °C.

Figure 3A shows the expanded view of the symmetric COO^- stretching region of the spectra with the 1st to 12th flashes (black for flashes 1−4, red for flashes 5−8, and blue for flashes 9−12). The spectral features at the $4n + 1$, $4n + 2$, $4n + 3$, and $4n + 4$ ($n = 1$ or 2) flashes resemble those of the 1st, 2nd, 3rd, and 4th flashes, respectively, although the intensities become smaller at later flashes, indicative of the presence of period four oscillation in the protein bands with some damping. The oscillation pattern was clearly seen in the flash-number dependence of the relative intensity (amplitude at the 1st flash adjusted to −1.0), estimated as an intensity difference between 1438 and 1400 cm^{-1}, at which prominent positive and negative peaks, respectively, appear in the 1st-flash spectrum [Figure 3B (●)]. Note that oscillation takes place around zero because all the motions of protein moieties return back upon completion of the S-state cycle.

Simulation of this oscillation pattern of the protein change was performed with a conventional method assuming a single average miss probability (α). The fitting function was[42]

$$f[n+1] = (1-\alpha)\{A_1 p_1[n] + A_2 p_2[n] + A_3 p_3[n] - (A_1 + A_2 + A_3) p_0[n]\} + c \quad (n = 0 - 11)$$

where $f[n + 1]$ is a signal amplitude at the $(n + 1)$th flash, A_1−A_3 are the ΔA intensities in the $S_1 \rightarrow S_2$, $S_2 \rightarrow S_3$, and $S_3 \rightarrow S_0$ transitions, respectively, $p_0[n]$, $p_1[n]$, $p_2[n]$, and $p_3[n]$ are the populations of the S_0, S_1, S_2, and S_3 states after the nth flash, respectively, and c is an offset to correct a zero line. The intensity in the $S_0 \rightarrow S_1$ transition is expressed as $-(A_1 + A_2 + A_3)$, because the sum of the ΔA intensities of the four S-state transitions should be zero. Double-hit probabilities were not included in the analysis, because an ∼7 ns laser pulse was used for excitation to prevent double hits.[21] The populations of the S states after the $(n + 1)$th flash are expressed as

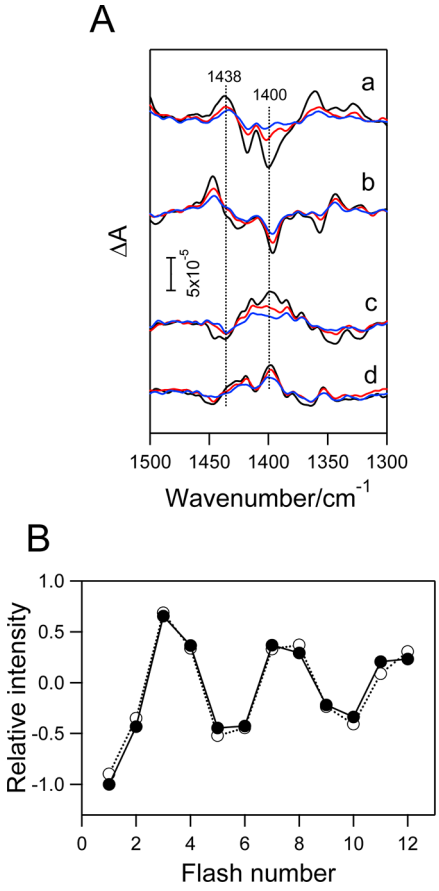

Figure 3. (A) Symmetric carboxylate stretching region of the FTIR difference spectra of the S-state cycle in the core complexes of *T. elongatus* WT′: (a) 1st, 5th, and 9th flashes, (b) 2nd, 6th, and 10th flashes, (c) 3rd, 7th, and 11th flashes, and (d) 4th, 8th, and 12th flashes. The black line denotes flashes 1−4, the red line flashes 5−8, and the blue line flashes 9−12. (B) Flash-number dependence of the relative amplitude of the protein signal (●) together with a simulated oscillation assuming a single miss probability (○). The signal amplitude was estimated as the intensity at 1400 cm^{-1} relative to that at 1438 cm^{-1} (indicated as dotted lines in panel A). The amplitude at flash 1 was adjusted to −1.0.

$$p_0[n+1] = \alpha p_0[n] + (1-\alpha)p_3[n]$$
$$p_1[n+1] = \alpha p_1[n] + (1-\alpha)p_1[n]$$
$$p_2[n+1] = \alpha p_2[n] + (1-\alpha)p_2[n]$$
$$p_3[n+1] = \alpha p_3[n] + (1-\alpha)p_3[n]$$

The initial populations before the 1st flash ($n = 0$) are $p_1[0] = 1$ and $p_0[0] = p_2[0] = p_3[0] = 0$, because of synchronization of the initial S states to S_1 by preflashes followed by dark incubation (see Materials and Methods). A good fitting was achieved as shown in Figure 3B (○). The average miss α was estimated to be 9.2 ± 1.4 (Table 1), which is similar to the previous results.[19,20,24,42] It is noted that using the protein signals, the miss probabilities of individual transitions cannot be estimated because of the unknown intensity parameters, A_1, A_2, and A_3. There is no unique solution in the simulation if both the miss probabilities and the signal intensities of individual transitions are changed as fitting parameters. In our previous FTIR study,[62] in which the effect of the extent of hydration of the PSII sample on the efficiencies (or miss probabilities) of the individual transitions was examined, we first assumed that the 1st, 2nd, 3rd, and 4th flash spectra of a fully hydrated PSII film were standard FTIR spectra representing the $S_1 \rightarrow S_2$, $S_2 \rightarrow S_3$, $S_3 \rightarrow S_0$, and $S_0 \rightarrow S_1$ transitions, respectively, and then estimated the relative efficiencies of the individual transitions in less hydrated films with respect to those in the standard fully hydrated sample by spectral fitting. Thus, absolute miss probabilities of the individual transitions have not been obtained in previous FTIR studies.

Table 1. Miss Probabilities (%) of the S-State Transitions Estimated Using Ferricyanide/Ferrocynaide and Protein FTIR Signals[a]

	T. elongatus PSII core complex			
	WT′	D2-Y160F	with NO_3^-	spinach PSII membranes
$S_0 \rightarrow S_1$	5.0 ± 2.7	4.6 ± 1.9	6.3 ± 3.5	6.1 ± 2.3
$S_1 \rightarrow S_2$	5.1 ± 3.8	5.2 ± 3.5	10.8 ± 4.7	17.6 ± 5.4
$S_2 \rightarrow S_3$	6.9 ± 4.0	9.0 ± 3.6	10.9 ± 4.9	20.8 ± 3.6
$S_3 \rightarrow S_0$	10.3 ± 4.1	13.3 ± 3.5	29.1 ± 6.0	26.7 ± 4.0
average[b]	6.8 ± 3.6	8.0 ± 3.1	14.3 ± 4.8	17.8 ± 3.8
protein[c]	9.2 ± 1.4	9.8 ± 1.7	14.5 ± 2.5	16.7 ± 3.1

[a]FTIR spectra were measured at 10 °C. [b]Average of miss probabilities of the four transitions estimated using a ferricyanide/ferrocyanide signal. [c]Miss probability estimated using protein bands assuming a single miss for all four transitions.

Figure 4A shows the ferricyanide/ferrocyanide bands in the flash-induced FTIR difference spectra of the WT′ core complexes upon the 1st to 4th (black lines), 5th to 8th (red lines), and 9th to 12th (blue lines) flashes. It is seen that the intensity of the ferricyanide/ferrocyanide signal slightly changes depending on the flash number. Except for the 1st flash, the 3rd, 7th, and 11th flashes induced signal intensities slightly smaller than those of other flashes in the same row. This relationship was well expressed in the plot of the flash-number dependence of the relative intensities [an averaged intensity was adjusted to 1.0 (see Materials and Methods)] of the ferricyanide/ferrocyanide signal presented in Figure 4B (●). The specifically low intensity at the 1st flash is ascribed to the $Fe^{3+} \rightarrow Fe^{2+}$ reduction of the non-heme iron preoxidized in some centers[63] instead of reduction of ferricyanide. Preflash illumination reduces the non-heme iron in all centers, but it may be partially reoxidized by ferricyanide during dark incubation for 30 min. A period four oscillation of the ferricyanide/ferrocyanide intensities was clearly seen after the 2nd flash; the minima were observed at 4th, 8th, and 12th flashes, and maxima were at the 5th and 9th flashes [Figure 4B (●)].

Because the ferricyanide/ferrocyanide signal directly reveals the electron flow from the WOC to ferricyanide upon flash illumination, the signal intensity should reflect the advancement of the S-state transition in the WOC irrespective of the S states before illumination. Thus, by analyzing the oscillation pattern of the ferricyanide/ferrocyanide signal, we can estimate the probabilities of the individual S-state transitions. The flash-number dependence of the ferricyanide/ferrocyanide intensity after the 2nd flash [Figure 4B (●)] was fit with the function

$$g[n+1] = I\{(1-\alpha_1)p_1[n] + (1-\alpha_2)p_2[n] + (1-\alpha_3)p_3[n] + (1-\alpha_0)p_0[n]\} - bn \quad (n = 1-11)$$

dx.doi.org/10.1021/bi300708a | *Biochemistry* 2012, 51, 6776−6785

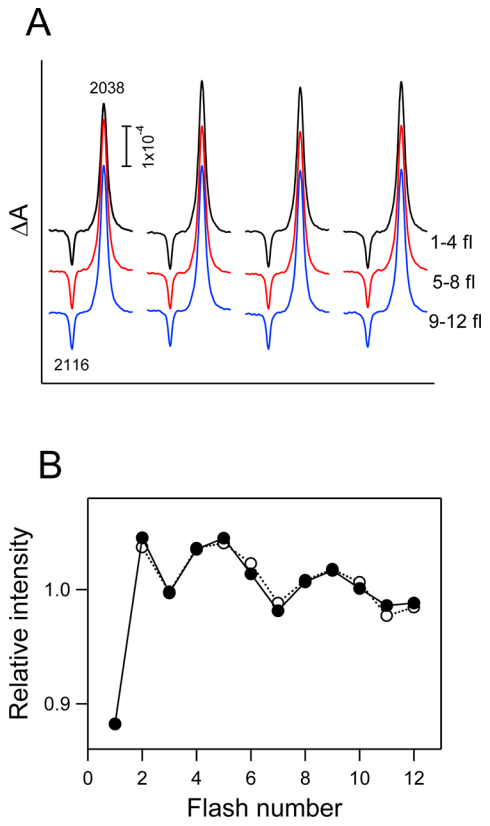

Figure 4. (A) CN stretching bands of ferricyanide (2116 cm^{-1}) and ferrocyanide (2038 cm^{-1}) in the FTIR difference spectra of the S-state cycle in the core complexes of *T. elongatus* WT′ at the 1st to 4th (black lines), 5th to 8th (red lines), and 9th to 12th (blue lines) flashes (from left to right, respectively). (B) Flash-number dependence of the relative amplitude of the ferricyanide/ferrocyanide bands (●) together with a simulated oscillation between the 2nd and 12th flashes (○). The amplitude of an averaged ferricyanide/ferrocyanide signal was adjusted to 1.0.

where $g[n + 1]$ is the intensity at the $(n + 1)$th flash, α_0–α_3 are the miss probabilities of the $S_0 \rightarrow S_1$, $S_1 \rightarrow S_2$, $S_2 \rightarrow S_3$, and $S_3 \rightarrow S_0$ transitions, respectively, I is an intensity parameter, and b is a parameter to correct a baseline slope. In the case of the WT′ data, the signal intensity gradually decreased with a larger flash number [Figure 4B (●)]. The reason for this baseline change is unknown at present. It could be caused by partial inactivation of centers by successive flash illumination. In some cases, however, the slope is positive like the data of NO_3^--treated PSII (see below), which cannot be explained by this model. Thus, it seems better to take this slope simply as one of fitting parameters for baseline correction.

The oscillation pattern of the ferricyanide/ferrocyanide signal was well simulated as presented in Figure 4B (○). The obtained miss parameters are summarized in Table 1. α_0–α_3 were estimated to be 5.0 ± 2.7, 5.1 ± 3.8, 6.9 ± 4.0, and 10.3 ± 4.1%, respectively. An average of these misses was 6.8 ± 3.6%, which is in fair agreement with the average miss estimated by protein bands (9.2 ± 1.4%) in the error range.

To examine the effect of Y_D on the miss probabilities, a similar experiment was performed using the PSII core complexes of the D2-Y160F mutant of *T. elongatus*, in which Y_D is replaced with Phe. If Y_D is in a reduced form, it can reduce the S_2 and S_3 states in seconds to contribute to the misses,[64,65] while if it is in an oxidized form, it can affect the kinetics of $P680^+$ to change the miss probabilities.[66] The oscillation pattern of the ferricyanide/ferrocyanide signal after the 2nd flash [Figure 5b (●)] was very similar to that of the WT′ strain

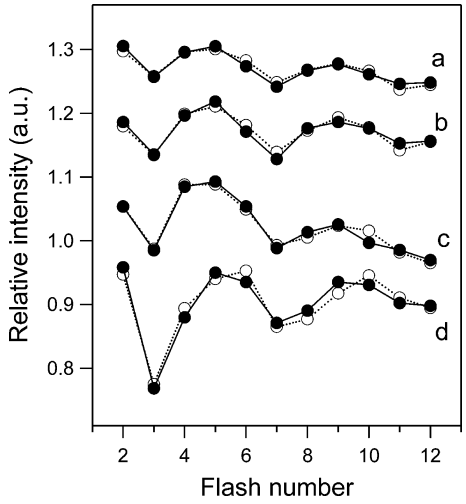

Figure 5. Oscillation patterns of the amplitude of the ferricyanide/ferrocyanide signal between the 2nd and 12th flashes (●) of the PSII core complexes of WT′ (a) and the Y_D-less (D2-Y160F) mutant (b) of *T. elongatus*, the PSII membranes of spinach (c), and the NO_3^--treated PSII core complexes of *T. elongatus* WT′ (d), together with simulated patterns (○).

[Figures 4B and 5a (●)]. Note that the initial state of the WOC in the D2-Y160F core was also synchronized to S_1 by two preflashes with subsequent dark incubation. Simulation of the oscillation pattern [Figure 5b (○)] provided the values of 4.6 ± 1.9, 5.2 ± 3.5, 9.0 ± 3.6, and 13.3 ± 3.5% as α_0–α_3, respectively (Table 1). The average miss was 8.0 ± 3.1%, which well agrees with the value of 9.8 ± 1.7% estimated from the protein bands (Table 1). The miss values mentioned above are in good agreement with those of WT′.

It should be noted that the above miss values of the $S_1 \rightarrow S_2$ and $S_2 \rightarrow S_3$ transitions involve the contribution of relaxation from the S_2 and S_3 states during the measurement time of 20 s, which was used to obtain an S/N ratio high enough for accurate analysis. We estimated the time constant of the S_3-state relaxation after two flashes under these sample conditions [200 mM Mes buffer (pH 6.0) in the presence of 100 mM ferricyanide] as $\tau \sim 20$ min by the experiments in which FTIR difference spectra upon two-flash illumination (1 Hz) were measured with different dark intervals. The S_3/S_1 difference spectrum has a negative intensity around 1400 cm^{-1}, but if the dark period is not enough to relax the S_3 state to the S_1 state through the S_2 state, the difference spectrum upon the next illumination involves the S_0/S_3 and S_1/S_0 differences with positive intensities around 1400 cm^{-1} and thus decreases the intensity. Using this relaxation time, it was estimated that 1–2% of centers relax from the S_3 and S_2 states during spectral accumulation for 20 s. Thus, true miss probabilities of the $S_1 \rightarrow S_2$ and $S_2 \rightarrow S_3$ transitions may be smaller by 1–2% than the estimated values. This correction implies that the miss probability of the $S_1 \rightarrow S_2$ transition may be very close to that of the $S_0 \rightarrow S_1$ transition, although the tendency of misses of individual S-state transitions is not much affected. Therefore, the results for the D2-Y160F mutant together with the data of WT′ showed that the miss probability of the $S_3 \rightarrow S_0$ transition is the largest, whereas the $S_0 \rightarrow S_1$ and $S_1 \rightarrow S_2$ transitions have

dx.doi.org/10.1021/bi300708a | *Biochemistry* 2012, 51, 6776–6785

similarly small miss probabilities. The miss probability of the $S_2 \rightarrow S_3$ transition has a medium value.

Measurements were also performed using PSII membranes from spinach (Figure 5c). Dips at the 3rd and 7th flashes seem to be larger than those of the core complexes of *T. elongatus* (Figure 5a,b). α_0–α_3 values were estimated to be 6.1 ± 2.3, 17.6 ± 5.4, 20.8 ± 3.6, and 26.7 ± 4.0%, respectively (Table 1). The average was 17.8 ± 3.8% in good agreement with the value of 16.7 ± 3.1% due to the protein bands. Thus, although the miss probabilities of the PSII membranes of spinach were generally larger than those of the core complexes of *T. elongatus*, the order among the miss probabilities ($\alpha_0 < \alpha_1 < \alpha_2 < \alpha_3$) was even more clearly revealed.

To demonstrate whether an influence of some perturbation to the WOC on the S-state transitions can be correctly estimated using our FTIR method, we applied the analysis described above to NO_3^--treated PSII core complexes of *T. elongatus*. The oscillation pattern of the ferricyanide/ferrocyanide signal [Figure 5d (●)] showed that the signal intensity at the 3rd flash was significantly reduced. The simulation of the oscillation [Figure 5d (○)] provided α_0–α_3 values of 6.3 ± 3.5, 10.8 ± 4.7, 10.9 ± 4.9, and 29.1 ± 6.0%, respectively (Table 1). The average of these values was 14.3 ± 4.8%, basically identical to α by protein analysis (14.5 ± 2.5%). Thus, it was clearly shown that NO_3^- treatment mainly increased α_3.

The estimated miss probabilities of individual S-state transitions of the four different samples are summarized in Figure 6, which shows a general tendency of miss probabilities in the order $\alpha_0 \leq \alpha_1 < \alpha_2 < \alpha_3$ and the specific increase in α_3 by NO_3^- treatment.

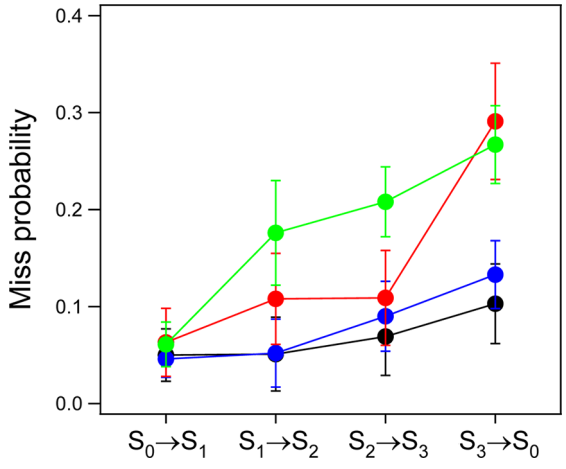

Figure 6. Estimated miss probabilities of the individual S-state transitions in the PSII core complexes of WT′ (black) and the Y_D-less (D2-Y160F) mutant (blue) of *T. elongatus*, the PSII membranes of spinach (green), and the NO_3^--treated PSII core complexes of *T. elongatus* WT′ (red). Error bars are standard deviations of the miss parameters estimated in simulations of the oscillation patterns.

DISCUSSION

In this study, FTIR spectroscopy was used to determine the miss probabilities of individual transitions in the S-state cycle of photosynthetic water oxidation. Ferricyanide was added to a PSII sample as a sole exogenous electron acceptor, and the S-state cycle was advanced by successive saturating flashes with an ~7 ns width, which prevents double hits. The electron flow from the WOC to ferricyanide upon each flash was monitored by detecting the CN stretching bands of ferricyanide (2116 cm^{-1}) and ferrocyanide (2038 cm^{-1}). Because the signal of the ferricyanide/ferrocyanide redox couple is totally independent of the S-state status in the WOC, the signal intensity directly reflects the extent of the electron flow in PSII, which corresponds to the advancement of the S-state transitions. Simulation of the oscillation pattern of the signal intensity provided individual miss probabilities without any assumptions in parameters (Figure 5).

The merits of this FTIR method to estimate miss probabilities are as follows. (1) The CN bands of ferricyanide and ferrocyanide appear at 2116 and 2038 cm^{-1}, respectively, in a specific region where any other components in the sample such as proteins and water do not show bands (Figure 2). Thus, without any interference from other infrared bands, the extent of the ferricyanide/ferrocyanide reaction can be accurately estimated. (2) In the presence of ferricyanide, Q_A and Q_B are always in their oxidized forms before each flash illumination, and hence, there is no complexity of the difference in the redox state on the acceptor side (Q_B or Q_B^-), which otherwise will provide different oscillation patterns in the S-state cycle due to the $Q_A^-Q_B \leftrightarrow Q_AQ_B^-$ equilibrium and the change in kinetics.[23] Thus, the original properties of the S-state transitions in the WOC independent of the acceptor side status can be estimated. (3) In the FTIR difference spectra of the S-state cycle, protein bands of the WOC are also detected below 1800 cm^{-1} in the same experiment (Figures 2 and 3A). These protein bands can be used to estimate an average miss probability (Figure 3B),[36,37,42] which is a good confirmation of individual miss probabilities estimated by the ferricyanide/ferrocyanide signal.

In the simulation analysis of the oscillation, the 1st flash data were eliminated because in some centers the non-heme iron is preoxidized and accepts an electron at the 1st flash (Figure 4B).[63] The fitting analysis of the oscillation patterns of the ferricyanide/ferrocyanide amplitudes of the PSII core complexes of the WT′ species (Figure 5a) and the Y_D-less (D2-Y160F) mutant (Figure 5b) of *T. elongatus* and the PSII membranes of spinach (Figure 5c) showed a general tendency that the miss probabilities are in the order $\alpha_0 \leq \alpha_1 < \alpha_2 < \alpha_3$ (Table 1 and Figure 6). The average probabilities were identical within the error range to those estimated from the protein bands of the WOC (Figure 3A and Table 1), confirming that this method using the ferricyanide/ferrocyanide signal on the electron acceptor side correctly estimated the probabilities of the WOC reactions on the donor side. The very similar miss values between the WT′ and Y_D-less PSII samples (average misses are 6.8 ± 3.6 and 8.0 ± 3.1%, respectively) indicate that there is almost no effect of Y_D on the estimated misses. Probably, Y_D was already oxidized by preillumination, and hence, fast relaxation of the S_2 and S_3 states by electron transfer from reduced Y_D[64,65] did not take place. This result also implies that the effect of a positive charge around $Y_D^\bullet$ on the redox equilibrium among P680, Y_Z, and the WOC[66] is not so large to change miss probabilities.[19,46,67]

On the electron donor side of PSII, there are secondary electron transfer pathways including β-carotene, Chl_Z, and cytochrome b_{559}.[68,69] The ferricyanide/ferrocyanide signal would appear, even if an electron is abstracted from these redox components but not from the WOC. In the presence of ferricyanide, however, cytochrome b_{559} is already oxidized and hence should not be involved in the reactions in these experiments. In addition, no FTIR signals typical of Chl_Z^+/Chl_Z[70] at 1714/1684 cm^{-1} and β-carotene$^+$/β-carotene[71] at

dx.doi.org/10.1021/bi300708a | *Biochemistry* 2012, 51, 6776–6785

1465, 1441, and 1148 cm^{-1} have not been detected in the FTIR difference spectra of each flash illumination (Figure 2) and even the difference spectra between before and after illumination of 12 successive flashes (data not shown but see Figure 1 of ref 42 in which a similar experiment was performed). Together with the very similar average misses estimated by the ferricyanide/ferrocyanide signal and the protein bands of the WOC (Table 1), this result indicates that the contribution of the secondary electron transfer pathways on the donor side to the estimated misses, if any, is trivial.

So far, there have been two experimental reports of estimation of miss probabilities of individual S-state transitions. De Wijn and van Gorkom[24] estimated the miss probabilities using spinach thylakoids by measuring fluorescence yield. Although the analysis in this method required some assumptions in parameters related to fluorescence and a miss contribution associated with Q_B^-, they showed that the relative amplitudes of the four misses are in the order $\alpha_0 < \alpha_1 < \alpha_2 < \alpha_3$, in which the $S_3 \rightarrow S_0$ transition has the highest miss probability. In contrast, the recent EPR study by Han et al.,[25] in which the populations of S states in PSII membranes after illumination of 0−6 flashes were directly quantified with EPR signals specific to individual S states, showed that the $S_2 \rightarrow S_3$ transition has the largest miss probability (23 and 16% at 1 and 20 °C, respectively), whereas the $S_3 \rightarrow S_0$ transition has a relatively small miss probability (7 and 3% at 1 and 20 °C, respectively). Our estimation of miss probabilities by the FTIR method using the core complexes of *T. elongatus* and the PSII membranes of spinach was in good agreement with the estimation by fluorescence; we found a general tendency of miss probabilities as $\alpha_0 \leq \alpha_1 < \alpha_2 < \alpha_3$ with the largest miss probability in the $S_3 \rightarrow S_0$ transition (Table 1 and Figure 6). The consistency with the fluorescence study using different sample conditions strongly supports our results of the estimation of individual miss probabilities.

On the other hand, the estimation by EPR[25] was significantly different from that by both fluorescence and FTIR methods. This discrepancy may not originate from the difference in samples and temperatures. We also used PSII membranes of spinach as in the EPR study, and the temperature was 10 °C, the middle of the 1−20 °C range in the EPR study. However, a clear difference exists in exogenous electron acceptors, i.e., ferricyanide in our experiments versus phenyl-*p*-benzoquinone (P*p*BQ) in the EPR study. Because the fluorescence study[24] did not use any exogenous electron acceptors because of thylakoids as a sample and showed results similar to those of our FTIR study, it could be possible that P*p*BQ is responsible for the discrepancy. When P*p*BQ is used as an electron acceptor, the oxidation state of the non-heme iron shows a period two oscillation; it is oxidized to Fe^{3+} by a P*p*BQ^- radical anion after odd-number flashes and then functions as an endogenous electron acceptor at even-number flashes.[72] Because the rate of transfer of electrons from Q_A to Fe^{3+} is much faster (less than ~20 μs[72]) than that from Q_A to Q_B (200−400 μs[73]), the 2nd and 4th flashes, to which the $S_2 \rightarrow S_3$ and $S_0 \rightarrow S_1$ transitions, respectively, mainly contribute, may provide smaller miss probabilities if the reactions on the electron acceptor side significantly affect the miss probabilities. However, the result of the EPR study[25] was opposite to this assumption and showed larger misses in the $S_2 \rightarrow S_3$ and $S_0 \rightarrow S_1$ transitions than in other two transitions at both 1 and 20 °C. Thus, the difference of the electron acceptor also does not seem to be a direct cause of the discrepancy. Further careful studies would be necessary to understand the reason for the different miss probabilities estimated using different spectroscopic methods.

The misses of the S-state transitions arise mainly from $P680^+Q_A^-$ recombination,[19,23,24,26] which occurs in the time region of 100−200 μs.[26,74] The general tendency of higher miss probabilities for higher S states of the WOC observed in this study is reasonable when considering the redox equilibrium among P680, Y_Z, and the WOC. The higher oxidation state of the Mn_4CaO_5 cluster should shift the equilibrium to the P680 side.[24] The largest miss probability in the $S_3 \rightarrow S_0$ transition is consistent with the previous observation of a large extent of microsecond components in the $P680^+$ reduction kinetics in the $S_3 \rightarrow S_0$ transition.[74] The presence of an ~200 μs "lag phase" before the transfer of an electron from the Mn_4CaO_5 cluster to $Y_Z^{\bullet}$[30,32,40] may also contribute to the large miss probability of the $S_3 \rightarrow S_0$ transition. During this lag phase, $Y_Z^{\bullet}$ should be in a redox equilibrium with $P680^+$, facilitating recombination with Q_A^- on a 100−200 μs time scale.

Because in the presence of ferricyanide, Q_B stays in the oxidized form before flash illumination, the lifetime of Q_A^- depends on only the rates of flow of electrons from Q_A^- to ferricyanide in a direct way or through Q_B. A recent time-resolved infrared study using the core complexes of *T. elongatus* showed that in some centers Q_A^- was reoxidized directly by ferricyanide in less than ~20 μs, while in other centers, it was reduced by Q_B in 300−500 μs (Supporting Information of ref 40). The higher miss probabilities in the PSII membranes of spinach than in the core complexes of *T. elongatus* [average misses of 17−18 and 7−10% for spinach and *T. elongatus*, respectively (Table 1)] may be ascribed to the difficulty in direct electron abstraction by ferricyanide because of the lower accessibility of ferricyanide to the vicinity of the Q_A site in the membrane preparations. In fact, a previous FTIR study using spinach PSII membranes in the presence of P*p*BQ as an electron acceptor showed a smaller average miss of ~7%.[75] Thus, this method using ferricyanide to monitor the electron flow seems to be more effective for the core complexes than membrane preparations, although even in the latter case, this method will provide important information about the relationship of individual misses.

It has been known that NO_3^- treatment of PSII preparations affects the $S_3 \rightarrow S_0$ transition by replacing Cl^- with NO_3^-.[43,44] We utilized this treatment to demonstrate the effectiveness of this FTIR method to assess the influence of some treatment on individual miss probabilities. The result clearly showed that NO_3^- treatment of the PSII core complexes of *T. elongatus* significantly increased the miss probability of the $S_3 \rightarrow S_0$ transition from 10 to 29%, whereas the miss probabilities of the other transitions were not much affected (Figures 5d and 6 and Table 1). This observation is consistent with the previous data showing inactivation of the S_3 state by NO_3^- to change the oscillation pattern,[44] indicating that this method correctly estimates the change in the miss probability of each S-state transition.

In conclusion, we have developed a new method for estimating the miss probabilities of individual S-state transitions by utilizing a ferricyanide/ferrocyanide signal in flash-induced FTIR difference spectra. It was shown that the transitions from higher S states have higher miss probabilities; that is, the $S_3 \rightarrow S_0$ transition has the largest miss probability. It was also demonstrated that this method is useful for studying the changes in miss probabilities by some perturbation on PSII, such as treatment of inhibitors or introduction of site-directed

mutations. Thus, this FTIR method will be useful for the detailed analysis of various spectroscopic data revealing kinetics and structural changes during the S-state cycle aiming at the elucidation of the molecular mechanism of photosynthetic water oxidation.

AUTHOR INFORMATION

Corresponding Author

*Phone: +81-52-789-2881. Fax: +81-52-789-2883. E-mail: tnoguchi@bio.phys.nagoya-u.ac.jp.

Funding

This study was supported by the Grants-in-Aid for Scientific Research from the Ministry of Education, Culture, Sports, Science and Technology (21370063, 23108706, and 23657099 to T.N.) and the JST-PRESTO program (4018 to M.S.).

Notes

The authors declare no competing financial interest.

ACKNOWLEDGMENTS

We thank Ms. Megumi Tomita for technical assistance in the experiments with PSII membranes from spinach.

ABBREVIATIONS

FTIR, Fourier transform infrared; Mes, 2-(*N*-morpholino)-ethanesulfonic acid; P680, special pair chlorophylls in photosystem II; Pheo, pheophytin electron acceptor of photosystem II; PSII, photosystem II; Q_A, primary quinone electron acceptor; Q_B, secondary quinone electron acceptor; WOC, water oxidizing center; Y_D, redox-active tyrosine on the D2 subunit (D2-Y160) in photosystem II; Y_Z, redox-active tyrosine on the D1 subunit (D1-Y161) in photosystem II.

ADDITIONAL NOTE

[a]The CN band of ferrocyanide sometimes shows a subpeak at ~2060 cm^{-1} of unknown origin in a hydrated film as a sample form (footnote 3 of ref 62). In such a case, however, a negative ferricyanide peak, which is insensitive to sample conditions, can be used for estimation of a ferricyanide reaction. The solution or pellet samples used in our study did not show such distortion of a ferrocyanide band.

REFERENCES

(1) Debus, R. J. (1992) The manganese and calcium ions of photosynthetic oxygen evolution. *Biochim. Biophys. Acta 1102*, 269–352.

(2) Hillier, W., and Messinger, J. (2005) Mechanism of photosynthetic oxygen production. In *Photosystem II: The Light-Driven Water:Plastoquinone Oxidoreductase* (Wydrzynski, T., and Satoh, K., Eds.) pp 567–608, Springer, Dordrecht, The Netherlands.

(3) McEvoy, J. P., and Brudvig, G. W. (2006) Water-splitting chemistry of photosystem II. *Chem. Rev. 106*, 4455–4483.

(4) Messinger, J., Noguchi, T., and Yano, J. (2011) Photosynthetic O_2 Evolution. In *Molecular Solar Fuels* (Wydrzynski, T., and Hillier, W., Eds.) Chapter 7, pp 163–207, Royal Society of Chemistry, Cambridge, U.K.

(5) Renger, G. (2012) Photosynthetic water splitting: Apparatus and mechanism. In *Photosynthesis: Plastid Biology, Energy Conversion and Carbon Assimilation* (Eaton-Rye, J. J., Tripathy, B. C., and Sharkey, T. D., Eds.) pp 359–414, Springer, Dordrecht, The Netherlands.

(6) Grundmeier, A., and Dau, H. (2012) Structural models of the manganese complex of photosystem II and mechanistic implications. *Biochim. Biophys. Acta 1817*, 88–105.

(7) Diner, B. A., and Rappaport, F. (2002) Structure, dynamics, and energetics of the primary photochemistry of photosystem II of oxygenic photosynthesis. *Annu. Rev. Plant Biol. 53*, 551–580.

(8) Renger, G., and Holzwarth, A. R. (2005) Primary electron transfer. In *Photosystem II: The Light-Driven Water:Plastoquinone Oxidoreductase* (Wydrzynski, T., and Satoh, K., Eds.) pp 139–175, Springer, Dordrecht, The Netherlands.

(9) Petrouleas, V., and Crofts, A. R. (2005) The quinone iron acceptor complex. In *Photosystem II: The Light-Driven Water:-Plastoquinone Oxidoreductase* (Wydrzynski, T., and Satoh, K., Eds.) pp 177–206, Springer, Dordrecht, The Netherlands.

(10) Ferreira, K. N., Iverson, T. M., Maghlaoui, K., Barber, J., and Iwata, S. (2004) Architecture of the photosynthetic oxygen-evolving center. *Science 303*, 1831–1838.

(11) Guskov, A., Kern, J., Gabdulkhakov, A., Broser, M., Zouni, A., and Saenger, W. (2009) Cyanobacterial photosystem II at 2.9-Å resolution and the role of quinones, lipids, channels and chloride. *Nat. Struct. Mol. Biol. 16*, 334–342.

(12) Umena, Y., Kawakami, K., Shen, J. R., and Kamiya, N. (2011) Crystal structure of oxygen-evolving photosystem II at a resolution of 1.9 Å. *Nature 473*, 55–60.

(13) Yano, J., Kern, J., Sauer, K., Latimer, M. J., Pushkar, Y., Biesiadka, J., Loll, B., Saenger, W., Messinger, J., Zouni, A., and Yachandra, V. K. (2006) Where water is oxidized to dioxygen: Structure of the photosynthetic Mn_4Ca cluster. *Science 314*, 821–825.

(14) Joliot, P., Barbieri, G., and Chabaud, R. (1969) Model of the System II photochemical centers. *Photochem. Photobiol. 10*, 309–329.

(15) Kok, B., Forbush, B., and McGloin, M. (1970) Cooperation of charges in photosynthetic O_2 evolution. I. A linear four step mechanism. *Photochem. Photobiol. 11*, 457–475.

(16) Joliot, P., and Kok, B. (1975) Oxygen evolution in photosynthesis. In *Bioenergetics of Photosynthesis* (Govindjee, Ed.) pp 387–412, Academic Press, New York.

(17) Forbush, B., Kok, B., and McGloin, M. (1971) Cooperation of charges in photosynthetic O_2 evolution. II. Damping of flash yield oscillation, deactivation. *Photochem. Photobiol. 14*, 307–321.

(18) Renger, G., and Hanssum, B. (1988) Studies on the deconvolution of flash-induced absorption changes into the difference spectra of individual redox steps within the water-oxidizing enzyme system. *Photosynth. Res. 16*, 243–259.

(19) Isgandarova, S., Renger, G., and Messinger, J. (2003) Functional differences of photosystem II from *Synechococcus elongatus* and spinach characterized by flash induced oxygen evolution patterns. *Biochemistry 42*, 8929–8938.

(20) Shinkarev, V. P. (2005) Flash-induced oxygen evolution in photosynthesis: Simple solution for the extended S-state model that includes misses, double-hits, inactivation, and backward-transitions. *Biophys. J. 88*, 412–421.

(21) Jursinic, P. (1981) Investigation of double turnovers in photosystem II charge separation and oxygen evolution with excitation flashes of different duration. *Biochim. Biophys. Acta 635*, 38–52.

(22) Delrieu, M. J. (1983) Evidence for unequal misses in oxygen flash yield sequence in photosynthesis. *Z. Naturforsch. C38*, 247–258.

(23) Shinkarev, V. P., and Wraight, C. A. (1993) Oxygen evolution in photosynthesis: From unicycle to bicycle. *Proc. Natl. Acad. Sci. U.S.A. 90*, 1834–1838.

(24) de Wijn, R., and van Gorkom, H. J. (2002) S-state dependence of the miss probability in Photosystem II. *Photosynth. Res. 72*, 217–222.

(25) Han, G., Mamedov, F., and Styring, S. (2012) Misses during water oxidation in photosystem II are S state-dependent. *J. Biol. Chem. 287*, 13422–13429.

(26) de Wijn, R., and van Gorkom, H. J. (2002) The rate of chargerecombination in Photosystem II. *Biochim. Biophys. Acta 1553*, 302–308.

(27) Christen, G., Reifarth, F., and Renger, G. (1998) On the origin of the '35-μs kinetics' of $P680^{+\bullet}$ reduction in photosystem II with an intact water oxidising complex. *FEBS Lett. 429*, 49–52.

(28) Dekker, J. P., Plijter, J. J., Ouwehand, L., and van Gorkom, H. J. (1984) Kinetics of manganese redox transitions in the oxygen-evolving apparatus of photosynthesis. *Biochim. Biophys. Acta 767*, 176−179.
(29) Renger, G., and Weiss, W. (1986) Studies on the nature of the water-oxidizing enzyme. III. Spectral characterization of the intermediary redox states in the water-oxidizing enzyme system Y. *Biochim. Biophys. Acta 850*, 184−196.
(30) Rappaport, F., Blanchard-Desce, M., and Lavergne, J. (1994) Kinetics of electron-transfer and electrochromic change during the redox transitions of the photosynthetic oxygen-evolving complex. *Biochim. Biophys. Acta 1184*, 178−192.
(31) Ono, T., Noguchi, T., Inoue, Y., Kusunoki, M., Matsushita, T., and Oyanagi, H. (1992) X-ray detection of the period-four cycling of the manganese cluster in photosynthetic water oxidizing enzyme. *Science 258*, 1335−1337.
(32) Haumann, M., Liebisch, P., Müller, C., Barra, M., Grabolle, M., and Dau, H. (2005) Photosynthetic O_2 formation tracked by time-resolved X-ray experiments. *Science 310*, 1019−1021.
(33) Babcock, G. T., Blankenship, R. E., and Sauer, K. (1976) Reaction kinetics for positive charge accumulation on water side of chloroplast photosystem II. *FEBS Lett. 61*, 286−289.
(34) Britt, R. D., Campbell, K. A., Peloquin, J. M., Gilchrist, M. L., Aznar, C. P., Dicus, M. M., Robblee, J., and Messinger, J. (2004) Recent pulsed EPR studies of the Photosystem II oxygen-evolving complex: Implications as to water oxidation mechanisms. *Biochim. Biophys. Acta 1655*, 158−171.
(35) Hillier, W., and Wydrzynski, T. (2001) Oxygen ligand exchange at metal sites: Implications for the O_2 evolving mechanism of photosystem II. *Biochim. Biophys. Acta 1503*, 197−209.
(36) Hillier, W., and Babcock, G. T. (2001) S-state dependent Fourier transform infrared difference spectra for the photosystem II oxygen evolving complex. *Biochemistry 40*, 1503−1509.
(37) Noguchi, T., and Sugiura, M. (2001) Flash-induced Fourier transform infrared detection of the structural changes during the S-state cycle of the oxygen-evolving complex in photosystem II. *Biochemistry 40*, 1497−1502.
(38) Debus, R. J., Strickler, M. A., Walker, L. M., and Hillier, W. (2005) No evidence from FTIR difference spectroscopy that aspartate-170 of the D1 polypeptide ligates a manganese ion that undergoes oxidation during the S_0 to S_1, S_1 to S_2, or S_2 to S_3 transitions in photosystem II. *Biochemistry 44*, 1367−1374.
(39) Kimura, Y., Mizusawa, N., Ishii, A., and Ono, T. (2005) FTIR detection of structural changes in a histidine ligand during S-state cycling of photosynthetic oxygen-evolving complex. *Biochemistry 44*, 16072−16078.
(40) Noguchi, T., Suzuki, H., Tsuno, M., Sugiura, M., and Kato, C. (2012) Time-resolved infrared detection of the proton and protein dynamics during photosynthetic oxygen evolution. *Biochemistry 51*, 3205−3214.
(41) Lavergne, J. (1991) Improved UV-visible spectra of the S-transitions in the photosynthetic oxygen-evolving system. *Biochim. Biophys. Acta 1060*, 175−188.
(42) Suzuki, H., Sugiura, M., and Noguchi, T. (2009) Monitoring proton release during photosynthetic water oxidation in photosystem II by means of isotope-edited infrared spectroscopy. *J. Am. Chem. Soc. 131*, 7849−7857.
(43) Sinclair, J. (1984) The influence of anions on oxygen evolution by isolated spinach chloroplasts. *Biochim. Biophys. Acta 764*, 247−252.
(44) Wincencjusz, H., Yocum, C. F., and van Gorkom, H. J. (1999) Activating anions that replace Cl^- in the O_2-evolving complex of photosystem II slow the kinetics of the terminal step in water oxidation and destabilize the S_2 and S_3 states. *Biochemistry 38*, 3719−3725.
(45) Sugiura, M., and Inoue, Y. (1999) Highly purified thermo-stable oxygen-evolving photosystem II core complex from the thermophilic cyanobacterium *Synechococcus elongatus* having His-tagged CP43. *Plant Cell Physiol. 40*, 1219−1231.
(46) Sugiura, M., Rappaport, F., Brettel, K., Noguchi, T., Rutherford, A. W., and Boussac, A. (2004) Site-directed mutagenesis of *Thermosynechococcus elongatus* photosystem II: The O_2 evolving enzyme lacking the redox active tyrosine D. *Biochemistry 43*, 13549−13563.
(47) Berthold, D. A., Babcock, G. T., and Yocum, C. F. (1981) A highly resolved, oxygen-evolving photosystem II preparation from spinach thylakoid membranes. EPR and electron-transport properties. *FEBS Lett. 134*, 231−234.
(48) Ono, T., and Inoue, Y. (1986) Effects of removal and reconstitution of the extrinsic 33, 24 and 16 kDa proteins on flash oxygen yield in photosystem II particles. *Biochim. Biophys. Acta 850*, 380−389.
(49) Noguchi, T. (2007) Light-induced FTIR difference spectroscopy as a powerful tool toward understanding the molecular mechanism of photosynthetic oxygen evolution. *Photosynth. Res. 91*, 59−69.
(50) Jones, L. H. (1963) Nature of bonding in metal cyanide complexes as related to intensity and frequency of infrared absorption spectra. *Inorg. Chem. 2*, 777−780.
(51) Noguchi, T., Ono, T., and Inoue, Y. (1995) Direct detection of a carboxylate bridge between Mn and Ca^{2+} in the photosynthetic oxygen-evolving center by means of Fourier transform infrared spectroscopy. *Biochim. Biophys. Acta 1228*, 189−200.
(52) Noguchi, T., and Sugiura, M. (2003) Analysis of flash-induced FTIR difference spectra of the S-state cycle in the photosynthetic water-oxidizing complex by uniform ^{15}N and ^{13}C isotope labeling. *Biochemistry 42*, 6035−6042.
(53) Kimura, Y., Mizusawa, N., Ishii, A., Yamanari, T., and Ono, T. (2003) Changes of low-frequency vibrational modes induced by universal ^{15}N- and ^{13}C-isotope labeling in S_2/S_1 FTIR difference spectrum of oxygen-evolving complex. *Biochemistry 42*, 13170−13177.
(54) Chu, H.-A., Hillier, W., and Debus, R. J. (2004) Evidence that the C-terminus of the D1 polypeptide of photosystem II is ligated to the manganese ion that undergoes oxidation during the S_1 to S_2 transition: An isotope-edited FTIR study. *Biochemistry 43*, 3152−3166.
(55) Debus, R. J. (2008) Protein ligation of the photosynthetic oxygen-evolving center. *Coord. Chem. Rev. 252*, 244−258.
(56) Noguchi, T. (2008) Fourier transform infrared analysis of the photosynthetic oxygen-evolving center. *Coord. Chem. Rev. 252*, 336−346.
(57) Noguchi, T., Inoue, Y., and Tang, X.-S. (1999) Structure of a histidine ligand in the photosynthetic oxygen-evolving complex as studied by light-induced Fourier transform infrared difference spectroscopy. *Biochemistry 38*, 10187−10195.
(58) Shimada, Y., Suzuki, H., Tsuchiya, T., Mimuro, M., and Noguchi, T. (2011) Structural coupling of an arginine side chain with the oxygen evolving Mn_4Ca cluster in photosynstem II as revealed by isotope-edited Fourier transform infrared spectroscopy. *J. Am. Chem. Soc. 133*, 3808−3811.
(59) Noguchi, T., and Sugiura, M. (2002) FTIR detection of water reactions during the flash-induced S-state cycle of the photosynthetic water-oxidizing complex. *Biochemistry 41*, 15706−15712.
(60) Chu, H.-A., Sackett, H., and Babcock, G. T. (2000) Identification of a Mn-O-Mn cluster vibrational mode of the oxygen-evolving complex in photosystem II by low-frequency FTIR spectroscopy. *Biochemistry 39*, 14371−14376.
(61) Kimura, Y., Ishii, A., Yamanari, T., and Ono, T. (2005) Water-sensitive low-frequency vibrations of reaction intermediates during S-state cycling in photosynthetic water oxidation. *Biochemistry 44*, 7613−7622.
(62) Noguchi, T., and Sugiura, M. (2002) Flash-induced FTIR difference spectra of the water oxidizing complex in moderately hydrated photosystem II core films: Effect of hydration extent on S-state transitions. *Biochemistry 41*, 2322−2330.
(63) Diner, B. A., and Petrouleas, V. (1987) Q_{400}, the non-heme iron of the Photosystem II iron-quinone complex. A spectroscopic probe of quinone and inhibitor binding to the reaction center. *Biochim. Biophys. Acta 895*, 107−125.
(64) Messinger, J., Schröder, W. P., and Renger, G. (1993) Structure-function relations in photosystem II. Effects of temperature and

chaotropic agents on the period four oscillation of flash-induced oxygen evolution. *Biochemistry 32*, 7658−7668.
(65) Vass, I., and Styring, S. (1991) pH-dependent charge equilibria between tyrosine-D and the S states in photosystem II. Estimation of relative midpoint redox potentials. *Biochemistry 30*, 830−839.
(66) Rutherford, A. W., Boussac, A., and Faller, P. (2004) The stable tyrosyl radical in Photosystem II: Why D? *Biochim. Biophys. Acta 1655*, 222−230.
(67) Jeans, C., Schilstra, M. J., Ray, N., Husain, S., Minagawa, J., Nugent, J. H. A., and Klug, D. R. (2002) Replacement of tyrosine D with phenylalanine affects the normal proton transfer pathways for the reduction of $P680^+$ in oxygen-evolving photosystem II particles from *Chlamydomonas*. *Biochemistry 41*, 15754−15761.
(68) Stewart, D. H., and Brudvig, G. W. (1998) Cytochrome b_{559} of photosystem II. *Biochim. Biophys. Acta 1367*, 63−87.
(69) Faller, P., Fufezan, C., and Rutherford, A. W. (2005) Side-path electron donors: Cytochrome b_{559}, chlorophyll Z and β-carotene. In *Photosystem II: The Light-Driven Water:Plastoquinone Oxidoreductase* (Wydrzynski, T., and Satoh, K., Eds.) pp 347−365, Springer, Dordrecht, The Netherlands.
(70) Noguchi, T., and Inoue, Y. (1995) Molecular interactions of the redox-active accessory chlorophyll on the electron-donor side of photosystem II as studied by Fourier transform infrared spectroscopy. *FEBS Lett. 370*, 241−244.
(71) Noguchi, T., Mitsuka, T., and Inoue, Y. (1994) Fourier transform infrared spectrum of the radical cation of β-carotene photoinduced in photosystem II. *FEBS Lett. 356*, 179−182.
(72) Diner, B. A., and Petrouleas, V. (1987) Q_{400}, the non-heme iron of the Photosystem II iron-quinone complex. A spectroscopic probe of quinone and inhibitor binding to the reaction center. *Biochim. Biophys. Acta 895*, 107−125.
(73) de Wijn, R., and van Gorkom, H. J. (2001) Kinetics of electron transfer from Q_A to Q_B in photosystem II. *Biochemistry 40*, 11912−11922.
(74) de Wijn, R., Schrama, T., and van Gorkom, H. J. (2001) Secondary stabilization reactions and proton-coupled electron transport in photosystem II investigated by electroluminescence and fluorescence spectroscopy. *Biochemistry 40*, 5821−5834.
(75) Suzuki, H., Taguchi, Y., Sugiura, M., Boussac, A., and Noguchi, T. (2006) Structural perturbation of the carboxylate ligands to the manganese cluster upon Ca^{2+}/Sr^{2+} exchange in the S-state cycle of photosynthetic oxygen evolution as studied by flash-induced FTIR difference spectroscopy. *Biochemistry 45*, 13454−13464.